Journal of the European Ceramic Society **10** (1992) 255–261

Consolidation of Y-TZP/SiC Particulate Composites by Sintering and Containerless Post-HIPing

Zh. Ding, R. Oberacker, H. Frei & F. Thümmler

Institut für Keramik im Maschinenbau, Zentrallaboratorium, Universität Karlsruhe (TH),
Haid-und-Neu-Str. 7, Postfach 6980, D-7500 Karlsruhe, Germany

(Received 16 December 1991; accepted 29 January 1992)

Abstract

The consolidation of ZrO_2–SiC particle composites was studied. Thermodynamical considerations show that the stability region can be extended to higher processing temperatures by adjusting the sintering atmosphere. Densification behaviour, phase composition and microstructure development of such composites during sintering in different gas mixtures out of the Ar–CO–SiO system was studied. A process consisting of pressureless sintering in controlled atmospheres and subsequent containerless post-HIPing was developed which allows full density processing of these materials with up to 30 vol.% SiC particles without any additional sintering additives.

Die Herstellung SiC-partikelverstärkter ZrO_2-Mischkeramiken wurde untersucht. Thermodynamische Überlegungen zeigen die Möglichkeit, daß der Stabilitätsbereich durch Kontrolle der Sinteratmosphäre zu höheren Temperaturen verschoben werden kann. In der vorliegenden Arbeit wurden das Verdichtungsverhalten, die Phasenstabilität und die Entwicklung des Mikrogefüges von SiC-partikelverstärkten Y-TZP-Keramiken untersucht. Ein Herstellungsverfahren wurde entwickelt, das aus druckloser Sinterung in kontrollierten Sinteratmosphären und anschließender kapselloser heißisostatischer Nachverdichtung besteht. Damit können ZrO_2/SiC-Mischkeramiken mit bis zu 30 vol.% SiC Partikeln ohne zusätzliche Sinterhilfsmittel vollständig verdichtet werden.

La consolidation des composites à matrice ZrO_2 et à dispersion de particules de SiC a été étudiée. L'examen thermodynamique montre que le domaine de stabilité peut être étendu à des températures de traitement thermique plus élevées par un choix judicieux de l'atmosphère de frittage. La densification, la composition cristallographique et le développement de la microstructure de ces composites ont été étudiés pour des frittages effectués sous différentes atmosphères appartenant au système Ar–CO–SiO. Un procédé, qui permet de densifier complètement des matériaux contenant jusqu'à 30% en volume de particules de SiC, sans aucun ajout d'additifs de frittage a été mis au point. Ce procédé consiste en un premier frittage conventionnel sous atmosphère contrôlée suivi d'une post-densification par pressage isostatique.

1 Introduction

Yttria-stabilized tetragonal zirconia polycrystals (Y-TZP) exhibit excellent mechanical properties, which are superior to other ceramic materials but only at ambient temperatures. With increasing temperature the properties of Y-TZP degrade drastically.[1,2] One alternative for the improvement of properties of Y-TZP at elevated temperatures is the addition of hard, high modulus materials.[3] The reinforcement of TZP with SiC whisker or fibre has therefore been studied by many investigators.[4–6] In comparison, the reinforcement with SiC particles has not been so intensively investigated. The advantages of SiC particles compared to whiskers are reduced toxicity and health problems. Additionally, normal ceramic powder processing can be used directly.

The consolidation of oxide–nonoxide ceramic composites, however, is often difficult, due to phase instabilities at the processing temperature. Therefore, full density processing requires axial hot pressing, encapsulated HIPing or sintering additives in most cases. The subject of this work is the development of a process consisting of pressureless

Journal of the European Ceramic Society 0955-2219/92/$5.00

sintering and subsequent containerless hot isostatic pressing for the fabrication of dense Y-TZP/SiC-particle composites.

2 Thermodynamical Considerations

The consolidation of oxide–nonoxide ceramic composites is difficult due to reactions between the components at moderate temperatures. For the system ZrO_2–SiC the relevant reaction is the formation of ZrC.[7–9]

$$ZrO_2 + 3/2SiC = ZrC + 3/2SiO + 1/2CO \quad (1)$$

The reaction is appreciable at temperatures above 1400°C in argon.[10] The gaseous reaction products SiO and CO generate pores in the specimen during sintering. Therefore it becomes impossible to consolidate the composites by pressureless sintering. Hot pressing or sintering additives were therefore used in most previous studies on ZrO_2/SiC-whisker composites. According to chemical principles the equilibrium of reactions with gaseous components can be influenced by controlling the sintering atmosphere. If the concentrations of CO and SiO in the atmosphere are high enough, the chemical equilibrium of reaction (1) would be shifted towards the left. So the stability region could be extended to higher processing temperatures.

In such atmospheres an additional problem arises from the decomposition of SiC:

$$SiC + CO = SiO + 2C \quad (2)$$

Therefore, the thermodynamic equilibria of reactions (1) and (2) must be simultaneously considered. The change of Gibbs' free energy (ΔG°_T) and equilibrium constant of a chemical reaction can be related as:

$$\Delta G^\circ_T = -RT\ln K_p \quad (3)$$

where R is the gas constant and T temperature in kelvin.

Assuming the activity coefficients to 1, the equilibrium constant of reactions (1) and (2) can be expressed as

$$K_{p,1} = (P_{SiO})^{3/2}(P_{CO})^{1/2} \quad (4)$$

and

$$K_{p,2} = P_{SiO}/P_{CO} \quad (5)$$

respectively.

Rearranging eqns (3) to (5) and defining $a = 2{\cdot}303R$ leads to the relationship of equilibrium partial pressures for reaction (1):

$$3\log(P_{SiO}) + \log(P_{CO}) = -\frac{2\Delta G^\circ_{T,1}}{aT} \quad (6)$$

and for reaction (2)

$$\log(P_{CO}) - \log(P_{SiO}) = \frac{\Delta G^\circ_{T,2}}{aT} \quad (7)$$

ΔG°_T of the reactions can be calculated from the Gibbs' function:

$$\Delta G^\circ_T = \Delta H^\circ_T - T\Delta S^\circ_T \quad (8)$$

ΔH and ΔS are here the change of enthalpy and entropy of the reactions, respectively. The calculated data are plotted in Fig. 1. The shaded field is the theoretical stable region in which ZrO_2 and SiC coexist at corresponding temperatures. Figure 1 makes it obvious that the stability region of the system ZrO_2–SiC can be extended to higher temperatures by variation in sintering atmosphere.

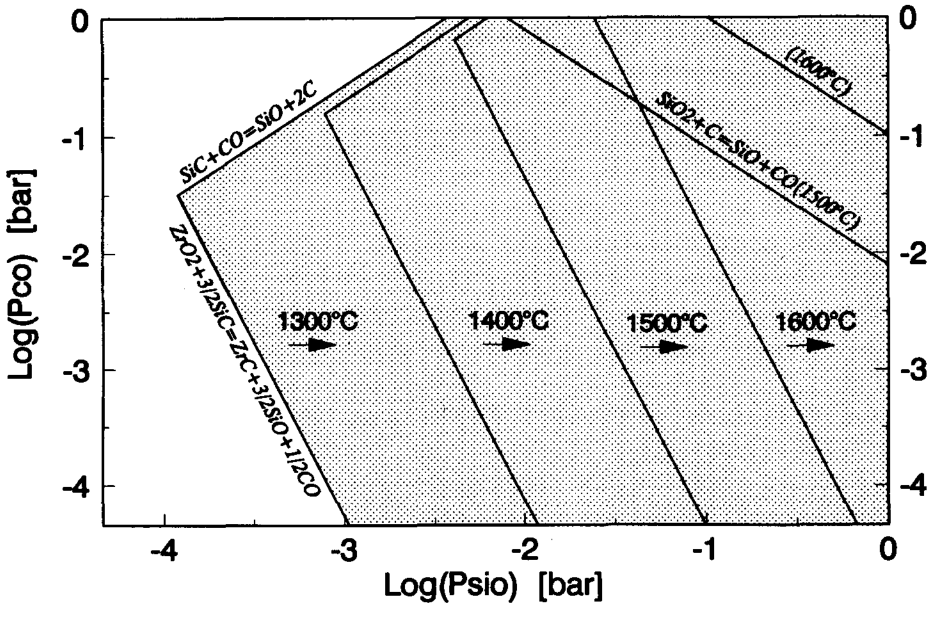

Fig. 1. Calculated equilibrium partial pressures of reactions (1) and (2) at various temperatures.

Table 1. Properties of the powders used

Material	d_{50} (*µm*)	*Specific surface area* (m^2/g)	Al_2O_3 (%)	SiO_2 (%)	Fe_2O_3 (%)	*C (free)* (%)	*Si (free)* (%)
TZ3Y	0·28	18·3	0·011	0·03	0·004	—	—
β-SiC	1·5	17·3	—	<0·6	—	<2·0	<0·1

3 Experimental Procedures

The starting materials used in this work were commercial ZrO_2 powder stabilized by 3 mol.% Y_2O_3 (TZ37; Toyo Soda Manufacturing Co., Ltd, Kanagawa, Japan) and β-SiC (Superior Graphite Co., Chicago, USA) powder. The property data given by the suppliers are shown in Table 1.

The powders were mixed in a attritor using ZrO_2 mill balls in a medium of isopropanol. After drying these mixtures in a rotary evaporator, they were die pressed with a pressure of 10 MPa and subsequently cold isostatically re-pressed at 400 MPa. The specimens were then pressureless sintered in a graphite furnace at temperatures ranging from 1350°C to 1650°C in controlled sintering atmospheres (flowing argon, Ar–CO and Ar–CO–SiO mixtures) for 0·5 to 2 h. Subsequently, the specimens were densified with a containerless post-HIPing process at 1450°C in Ar under 150 MPa for 0·5 h. The densification behaviour during sintering was measured by a dilatometer. The densities of sintered and post-HIPed specimens were measured by Archimedes' method. Microstructure was observed by TEM, phase analysis was carried out by X-ray diffraction. The ZrC content which formed during sintering was calculated from XRD reflexion intensity according to the following empirical equation:

$$\mathrm{ZrC} = \frac{I_{z(111)}}{I_{z,t(111)} + I_{z,m(\bar{1}11)} + I_{z(111)} + I_{s(111)}} \times f(\text{mass}\%)$$

Here, I_z, $I_{t.c}$, I_m and I_s are the X-ray reflexion intensities of corresponding lattice planes of ZrC, t-ZrO_2, m-ZrO_2 and SiC, respectively. f is an empiric correcting factor, which was estimated from calibration experiments with powder specimens to $f = 0{\cdot}745$.

4 Results and Discussion

4.1 Phase stability

Sintering of ZrO_2–SiC composites in argon led to appreciable formation of ZrC. Figure 2 illustrates the relationship between SiC content and the ZrC formation temperature. With increasing SiC content the ZrC formation temperature was lowered. The driving force of reaction (1) increases with temperature as shown in Fig. 3. At temperatures lower than 1600°C the specimens containing 40 vol.% SiC exhibit no significant densification. Sintering of this composition at 1650°C led to only 67% of theoretical density combined with strong ZrC formation. This means that pressureless sintering of ZrO_2–SiC composites in pure argon atmosphere is not possible without ZrC formation.

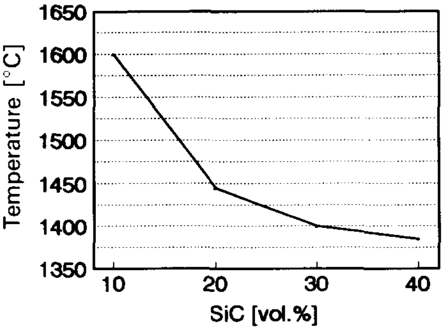

Fig. 2. ZrC formation temperatures during sintering of ZrO_2–SiC composites in argon (2 h).

The phase stability of ZrO_2–SiC composites during sintering was improved by using an Ar–CO gas mixture. Figure 4 shows the influence of CO additions to the flowing argon on the formation of ZrC in specimens with 20 vol.% SiC at 1550°C. Reaction (1) was suppressed by using an atmosphere consisting of argon and CO with 20 vol.% CO. However, reaction (2) was even enhanced. TEM

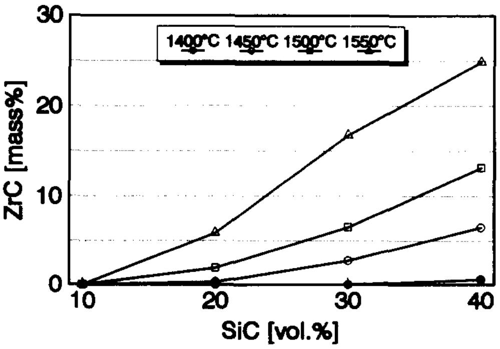

Fig. 3. Influence of sintering temperature on the formation of ZrC (sintered in argon, 2 h).

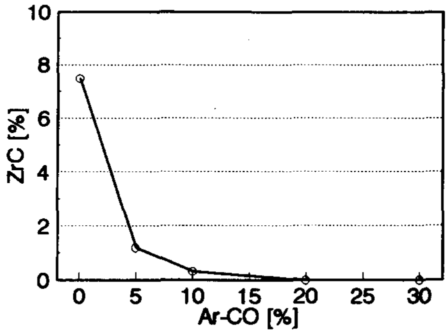

Fig. 4. Influence of CO additions on the formation of ZrC in the specimen of 3YTZP20SiC sintered in Ar–CO at 1550°C, 2 h.

observations showed free carbon with the shape of former SiC grains (marked C) in the specimens sintered in this atmosphere (Fig. 5). This limit is lower than that reported in Ref. 10, where SiC decomposes at CO contents of more than 33 vol.%. It is therefore evident that a SiO-containing atmosphere will be needed in order to prevent the decomposition of SiC.

A partial pressure of SiO in the sintering atmosphere can be realized through the partial reduction of SiO_2:

$$SiO_2 + CO = SiO + CO_2 \qquad (9)$$

Due to the use of a graphite heater and insulation, parts the following reaction must also be considered:

$$C + CO_2 = 2CO \qquad (10)$$

Rearranging reactions (9) and (10) leads to the following general reaction for the equilibrium of the system:

$$SiO_2 + C = SiO + CO \qquad (11)$$

The calculation is the same as previously and is also demonstrated in Fig. 1. From Fig. 1 it becomes obvious that the equilibrium partial pressure of SiO of reaction (11) falls just into the stability region. Therefore, the SiO partial pressure needed can be introduced by a SiO_2 powder bed. In the specimen with 30 vol.% SiC sintered in an Ar-20CO atmosphere containing SiO, free C was not found, i.e. an Ar–CO–SiO atmosphere is effective in suppressing the ZrC formation as well as the SiC decomposition during pressureless sintering of ZrO_2–SiC composites at elevated temperatures.

Additionally, no phase transformation from t-ZrO_2 to m-ZrO_2 during sintering in gas mixtures Ar–CO–SiO was observed in these materials.

4.2 Densification behaviour

Due to the generation of gaseous reaction products from reaction (1) during sintering the pressureless densification to pore closure of ZrO_2–SiC composites in argon is not possible. A sintering atmosphere containing CO suppresses ZrC formation and therefore improves the densification process, as demonstrated in Fig. 6. The more CO will be needed the higher the SiC content is. With increasing CO content in the atmosphere the sintering density increases. The density of the specimen with 20 vol.% SiC sintered in Ar–30 vol.% CO was lower than in Ar–20 vol.% CO. This can be explained by the decomposition of SiC following reaction (2), if the CO partial pressure is too high. Therefore, specimens containing 40 vol.% SiC could not be densified because in this case 40 vol.% CO will be needed to impede the ZrC formation.

Figure 7(a) shows the dilatometer studies of the specimens sintered in Ar and Ar–CO gas mixtures. Bimodal shrinkage rate profiles were observed. The difference in shrinkage behaviour occurs within the second maximum, which was much higher in Ar–CO gas mixtures than in pure argon. It seems that the reducing atmosphere improves the densification between the SiC grains.

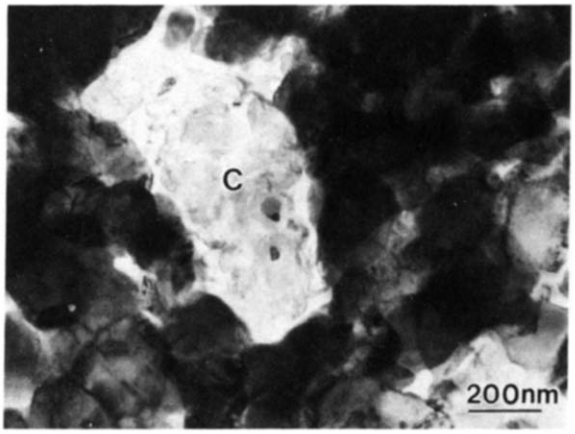

Fig. 5. Free C in the specimen of 3YTZP20SiC sintered in Ar-20CO at 1450°C, 2 h.

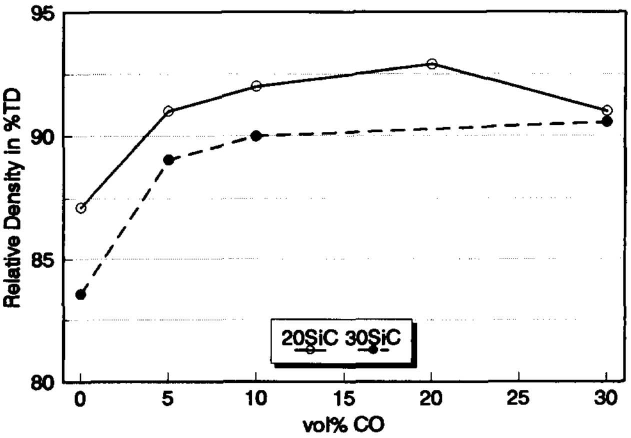

Fig. 6. Influence of CO on the densification of 3YTZP/SiC composites (sintered in Ar–CO at 1550°C, 2 h).

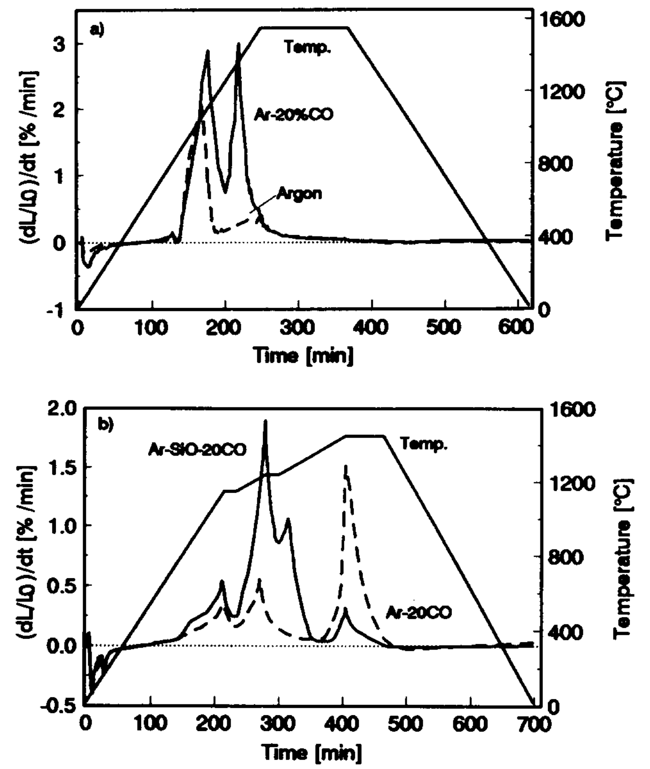

Fig. 7. Influence of CO and SiO on the densification of 3YTZP/SiC composites: (a) 3YTZP20SiC; (b) 3YTZP30SiC.

As already mentioned, SiC decomposes in atmospheres containing more than 20 vol.% CO. Hence, sintering atmospheres consisting of Ar, CO and SiO were used in order to suppress ZrC formation and SiC decomposition simultaneously. The results are shown in Table 2. It is obvious that a SiO-containing atmosphere results in a substantial increase of sintering density. It is supposed that the reduction of the SiO_2 film on SiC particles was impeded by SiO. SiO_2 acts then via liquid phase formation and improves the densification process. The densification behaviour measured by dilatometer (Fig. 7(b)) confirmed this assumption. The shrinkage rate at lower temperatures of the specimen sintered in Ar–SiO–20CO was much higher than that in Ar–20CO.

These experimental results confirmed the thermodynamic considerations. The region of coexistence of ZrO_2 and SiC can be extended to the processing temperatures required for reaching pore closure by pressureless sintering. Specimens sintered to closed porosity at 1450–1550°C in gas mixtures of Ar–SiO containing 20–30 vol.% CO were densified subsequently by containerless post-HIPing (1450°C, 150 MPa, 0·5 h), which allowed full densification of these materials with up to 30 vol.% SiC particles.

4.3 Microstructures

During sintering of ZrO_2–SiC composites in argon ZrO_2 reacts with SiC to ZrC. As demonstrated in Fig. 8 the newborn ZrC grains are very small with a grain size between 10 and 100 nm. In grain boundaries between ZrO_2 and SiC microcracks were induced by residual stresses, due to large differences in thermal expansion coefficients of the two components and restraining of the ZrO_2 matrix. An amorphous layer in the ZrO_2–SiC grain boundaries with a thickness of about 3 nm can be seen in Fig. 9. Probably the SiO_2 layer on SiC grains was not reduced under the sintering condition. In the specimens sintered in Ar–20CO neither ZrC nor amorphous phases were detected. The SiO_2 layer should be reduced by the strong reducing atmosphere, but, as already mentioned, SiC decomposes and free C is formed in this case.

The microstructure of the specimens sintered in

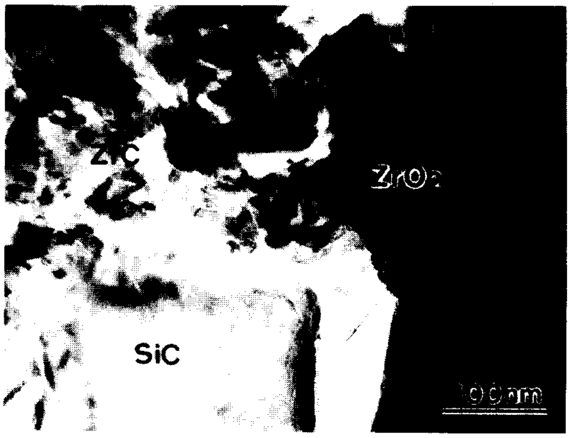

Fig. 8. Newborn ZrC during sintering of 3YTZP30SiC (1450°C, 2 h).

Table 2. Influence of SiO on the densification of ZrO_2–SiC composites

Composition	*Temperature (°C)*	*Atmosphere*	*Density (%TD)*	*Open porosity (%)*
3YTZP20SiC	1450°C	Ar–20CO	83·52	0·31
3YTZP20SiC	1450°C	Ar–SiO–20CO	91·01	0·15
3YTZP20SiC	1500°C	Ar–SiO–20CO	90·41	0·04
3YTZP30SiC	1450°C	Ar–20CO	78·85	18·57
3YTZP30SiC	1450°C	Ar–SiO–20CO	86·09	11·79
3YTZP30SiC	1500°C	Ar–SiO–20CO	89·00	0·79

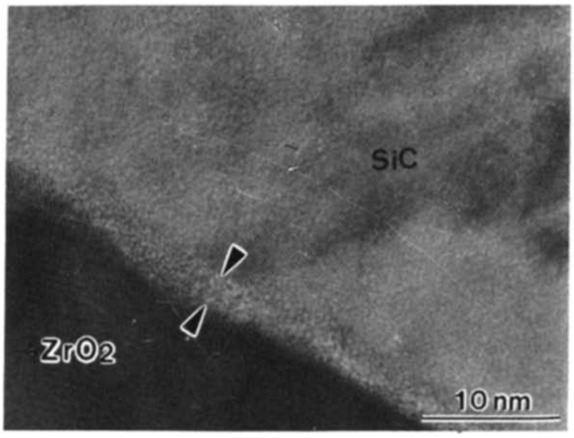

Fig. 9. Amorphous layer in grain boundary ZrO_2/SiC (Ar, 1450°C, 2 h).

atmospheres consisting of argon, CO and SiO showed differences to that of those sintered in atmospheres without SiO. Figure 10(a) shows a much smaller grain size than that sintered in Ar–CO–SiO (Fig. 10(b)). By TEM studies again an amorphous layer about 3 nm thick was observed along the grain boundaries of ZrO_2/SiC (Fig. 11). The SiO_2 layers on the SiC particles seem to have formed a liquid phase and promoted the grain growth, as was already indicated by the dilatometer experiments. The amorphous grain boundary phases are of course not desired because of the degrading high-temperature properties of ceramics.

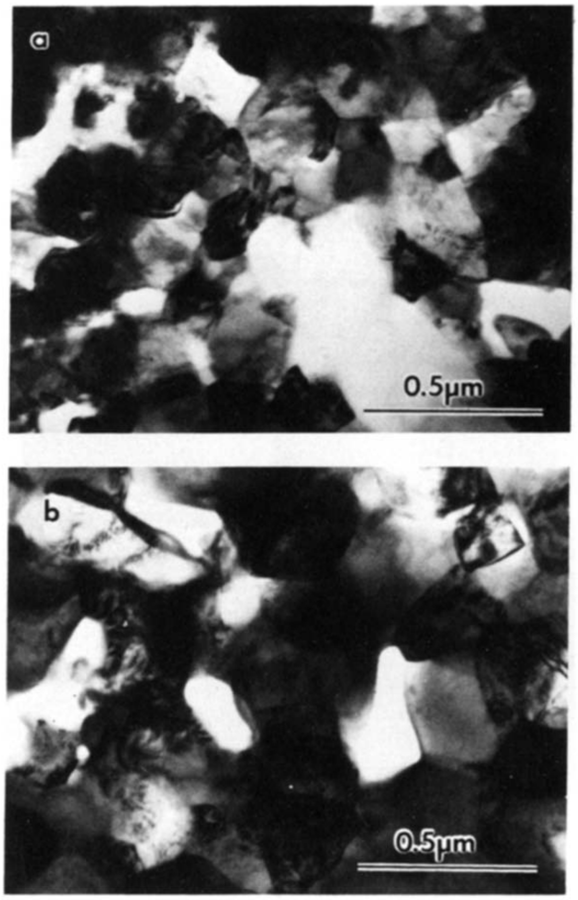

Fig. 10. Microstructure of 3YTZP30SiC composite sintered at 1550°C, 2 h in (a) Ar–20CO and (b) Ar–SiO–20CO.

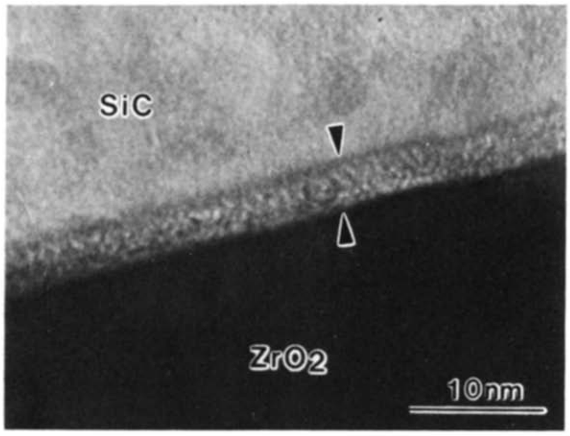

Fig. 11. Grain boundary phase in specimen of 3YTZP30SiC sintered in Ar–SiO–20CO at 1550°C, 2 h.

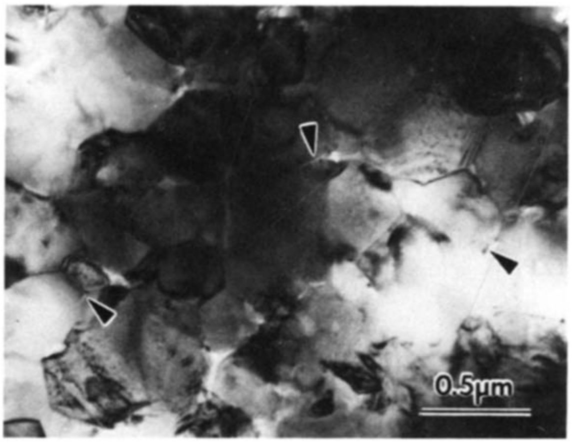

Fig. 12. Microcracks in specimen of 2YTZP20SiC sintered in Ar–SiO–20CO at 1450°C, 2 h, post-HIPed at 1450°C, 0·5 h.

In Fig. 12 the microstructure of a 100% dense specimen containing 20 vol.% SiC is demonstrated, which was sintered to pore closure in an Ar–SiO–CO gas mixture and fully densified by subsequent containerless post-HIPing. The grains are very small with grain sizes below 0·5 μm. Along the grain boundaries microcracks were detected (marked by arrows). This is probably one of the toughening mechanisms of this material.

5 Conclusions

(1) Sintering of ZrO_2/SiC composites to densities of technical interest in argon is not possible due to the instability of the phases.
(2) By adjusting the sintering atmosphere the densification of ZrO_2/SiC composites can be

improved. In Ar–CO atmospheres the formation of ZrC can be impeded, but the decomposition of SiC will be enhanced.

(3) In controlled sintering atmospheres consisting of argon, CO and SiO both the ZrC formation and the decomposition of SiC can be avoided. But an amorphous grain boundary layer, about 3 nm thick, between ZrO_2 and SiC was observed in specimens sintered in Ar and in Ar–CO–SiO. Their influence on the mechanical properties of ZrO_2/SiC requires further investigation.

(4) A process consisting of pressureless sintering in controlled atmospheres and subsequent containerless post-HIPing has been developed which allows full density processing of ZrO_2/SiC-particle composites containing up to 30 vol.% SiC.

References

1. Kobayashi, K., Kawajima, M. & Masaki, T., Phase change and mechanical properties of ZrO_2–Y_2O_3 solid electrolyte after aging. *Solid State Ionics*, **3/4** (1981) 489–95.
2. Iio, S., Watanabe, M., Sada, H. & Imura, T., Tetragonal to monoclinic transformation in Y-TZP during low temperature aging. In *Advances in Ceramics, Vol. 24A: Science and Technology of Zirconia III*, ed. S. Somiya, N. Yamamoto and H. Hanagida. American Ceramic Society, Inc., Westerville, OH, 1988, pp. 49–54.
3. Claussen, N., Strengthening strategies for ZrO_2-toughened ceramics at high temperatures. *Mat. Sci. Eng.*, **71** (1985) 23–38.
4. Faber, K. T., Intergranular crack-deflection toughening in silicon carbide. *J. Am. Ceram. Soc.*, **66** (1983) C94–C96.
5. Claussen, N., Weisskopf, K.-L. & Rühle, M., Tetragonal zirconia polycrystals reinforced with SiC whisker. *J. Am. Ceram. Soc.*, **69** (1986) 288–92.
6. Yasuda, E., Kimira, S., Katano, Y. & Akimune, Y., Mechanical properties of SiC whisker-reinforced PSZ. In *Advances in Ceramics, Vol. 24B: Science and Technology of Zirconia III*, ed. S. Somiya, N. Yamamoto & H. Hanagida. American Ceramic Society, Inc., Westerville, OH, 1988, pp. 701–8.
7. Omori, M., Takei, H. & Ohira, A., Synthesis of SiC–ZrO_2 composite containing t-ZrO_2. *J. Mat. Sci. Lett.*, **4** (1985) 770–2.
8. Lorenz, J., Lukas, H. L., Huke, E. E. & Gauckler, L. J., The stability of SiC-based ceramics containing ZrO_2 and other oxides. *CALPHD*, **7** (1983) 125–35.
9. Gauckler, L. J., Weiss, J. & Petzow, G., Stability of Si_3N_4- and SiC-based materials containing ZrO_2. In *Energy and Ceramics*, ed. P. Vincenzini. Elsevier Scientific Publishing Company, New York, 1980, pp. 671–9.
10. Mitsui, A. & Kato, A., Effect of carbon monoxide on the sintering of SiC whisker–ZrO_2 composites. *J. Ceram. Soc. Japan*, **95** (1987) 108–10.